Star Formation Newsletter
No. 343 27-33

高橋実道（NAOJ）

27 **Self-Sustaining Vortices in Protoplanetary Disks: Setting the Stage for Planetary System Formation**

Zsolt Regaly, Kundan Kadam, Cornelis P. Dullemond

28 **Physical conditions in the warped accretion disk of a massive star. 349 GHz ALMA observations of G023.01−00.41**

A. Sanna, A. Giannetti, M. Bonfand, L. Moscadelli, R. Kuiper, J. Brand, R. Cesaroni, A. Caratti o Garatti, T. Pillai, K. M. Menten

29 **FORCAST imaging of two small nearby Clusters: The Coronet and B59**

G. Sandell, B. Reipurth, W. D. Vacca, N. S. Bajaj

30 **Chandra X-ray Observations of V830 Tau: A T Tauri Star Hosting an Evanescent Planet**

Stephen L. Skinner, Manuel Guedel

31 **X-raying the Sco-Cen OB association: The low-mass stellar population revealed by eROSITA**

J. H. M. M. Schmitt, S. Czesla, S. Freund, J. Robrade, P. C. Schneider

32 **The filamentary structures in the CO emission toward the Milky Way disk**

J. D. Soler, H. Beuther, J. Syed, Y. Wang, Th. Henning, S. C. O. Glover, R. S. Klessen, M. C. Sormani, M. Heyer, R. J. Smith, J. S. Urquhart, J. Yang, Y. Su, X. Zhou

33 **The general applicability of self-similar solutions for thermal disc winds**

Andrew D. Sellek, Cathie J. Clarke, Richard A. Booth

27 **Self-Sustaining Vortices in Protoplanetary Disks: Setting the Stage for Planetary System Formation**

Zsolt Regaly, Kundan Kadam, Cornelis P. Dullemond

The core accretion scenario of planet formation assumes that planetesimals and planetary embryos are formed during the primordial, gaseous phases of the protoplanetary disk. However, how the dust particles overcome the traditional growth barriers is not well understood. The recently proposed viscous ring-instability may explain the concentric rings observed in protoplanetary disks by assuming that the dust grains can reduce the gas conductivity, which can weaken the magneto-rotational instability. We present an analysis of this model with the help of GPU-based numerical hydrodynamic simulations of coupled gas and dust in the thin-disk limit. During the evolution of the disk the dusty rings become Rossby unstable and break up into a cascade of small-scale vortices. The vortices form secularly stable dusty structures, which could be sites of planetesimal formation by the streaming instability as well as direct gravitational collapse. The phenomenon of self-sustaining vortices is consistent with observational constraints of exoplanets and sets a favorable environment for planetary system formation.

原始惑星系円盤での微惑星形成理論

Dullemond & Penzlin (2018)：viscous ring-instability (VRI)による円盤中でのダスト集積

VRI: MRI active な円盤で pressure bump が形成 →ダストが集積

→ 小さなダストは円盤のconductivity を下げる

→ MRI が抑制される→ よりダストを集積

VRIでリング状にダストを集積可能

この論文では、その後の進化をシミュレーションで調べる。

2D シミュレーション（GFARGO2）

α粘性モデルでVRIを再現

$$\alpha = \alpha_{\rm bg} \left(\frac{\Sigma_{\rm d}}{\Sigma_{\rm d}^0} \right)^{\phi_{\rm d}} \left(\frac{\Sigma_{\rm g}}{\Sigma_{\rm g}^0} \right)^{\phi_{\rm g}}$$

ダストサイズはSt = const で与える。

Model name	**St**	ϕ_g	ϕ_d	**Significance**
V1	0.1	1	-1	inner disk (fiducial)
V2	0.1	1	-1	outer disk
V3	0.1	1	-1	high metallicity
V1(St=1)	1	1	-1	grown dust
V1(St=0.01)	0.01	1	-1	small-sized dust
V1($\phi_g = -1$)	0.1	-1	-1	gas MHD effects

結果：VRIで形成されたリング構造が
ロスビー波不安定になり渦を形成

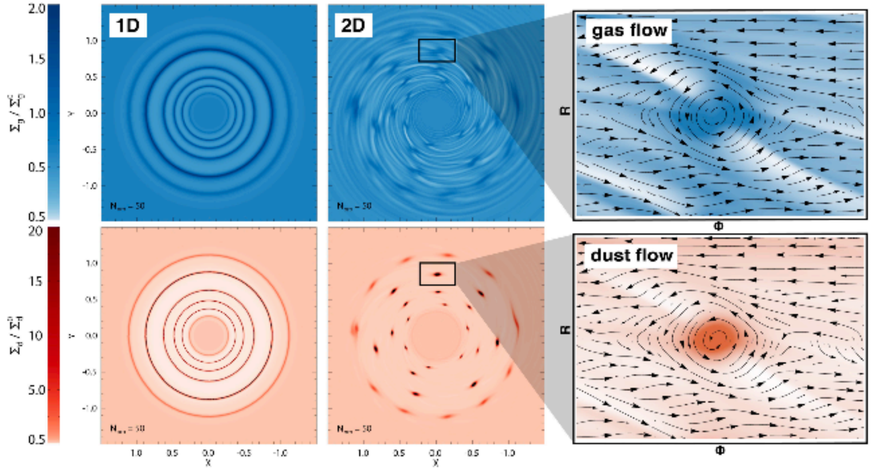

形成された渦は時間とともに落下。
αのダストガス比依存性により壊れない。
ガスの腕構造から、次の世代の渦が生まれる。

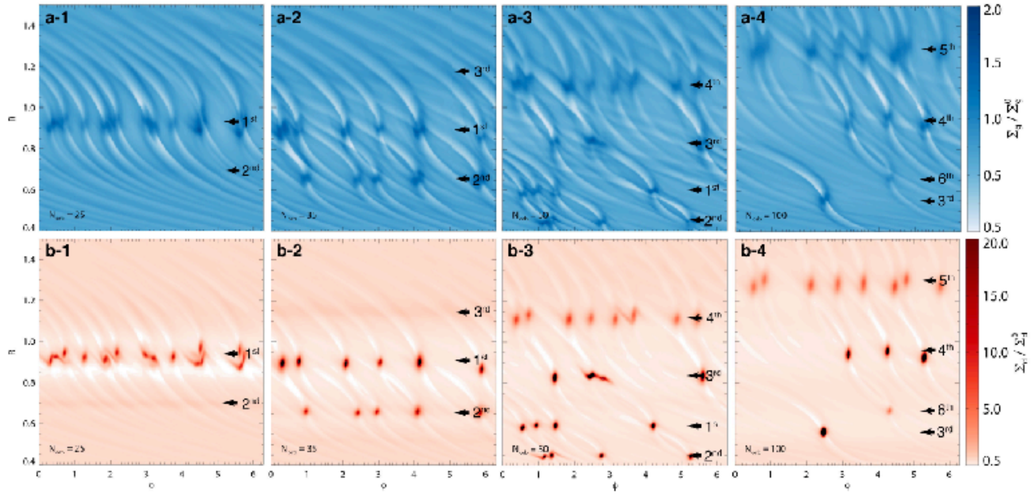

V1　（1au 付近）

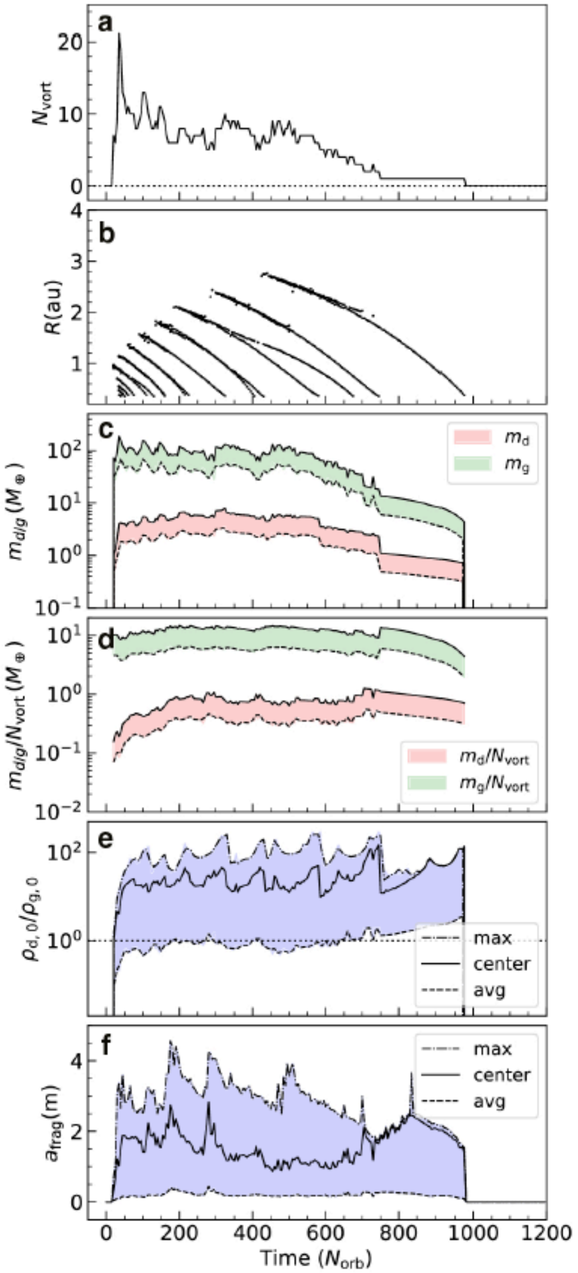

500周程度まで渦が形成、落下を繰り返す。
（ダストの落下で500周で止まる）

渦一個あたりのダスト質量は
時間とともに増加。> 0.1Me

ダストガス比は渦全体の平均でも
1を超える
→Streaming instability につながる

衝突破壊で決まるサイズを計算
→1mを超える微惑星が形成可能

V3　（ダストガス比x10）

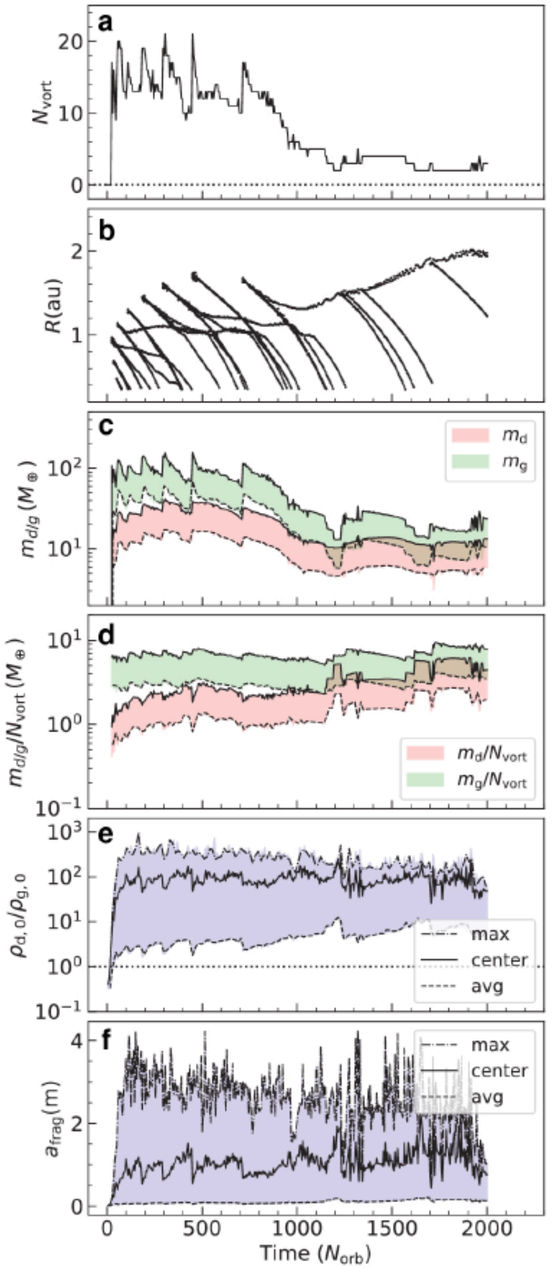

渦の分裂が見られる
分裂した渦が落下し、
元の渦は外側に移動する。

分裂片のダスト質量や
ダストガス比は
前のモデルの約10倍

分裂で決まるダストサイズ
は約２倍

V1($\phi_g = -1$)

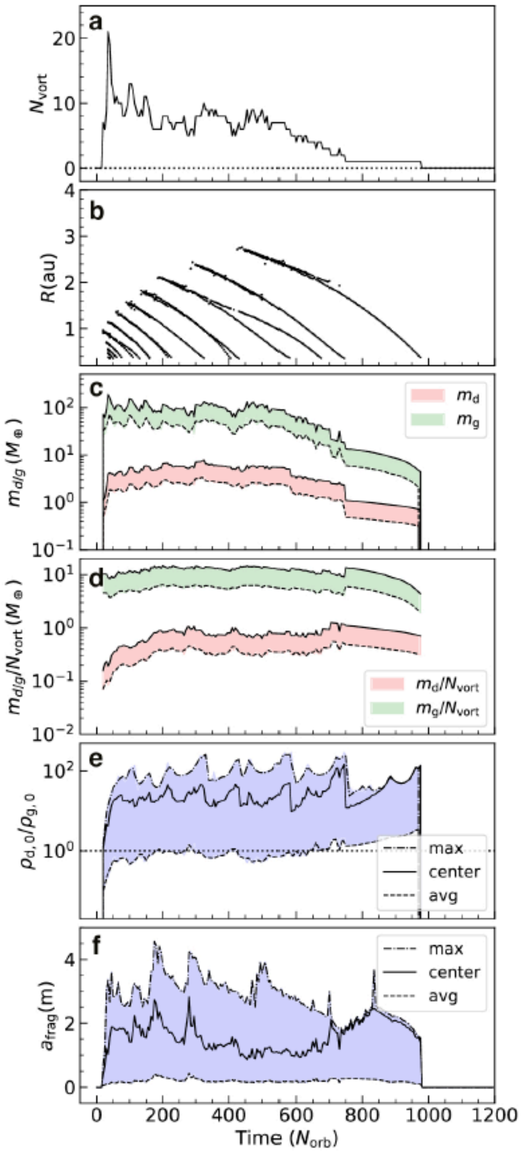

Non-Ideal MHDの局所計算では
低密度、高フラックスの領域と
高密度、低フラックスの領域が
できる(Zonal flow)
→低密度ではα大、高密度でα小
これを再現するモデルで計算

$$\alpha = \alpha_{bg} \left(\frac{\Sigma_d}{\Sigma_d^0} \right)^{\phi_d} \left(\frac{\Sigma_g}{\Sigma_g^0} \right)^{\phi_g}$$

このモデルでもVRI(?)での
リング形成、RWIの渦形成に至る

渦のダスト質量などの物理量は
もとのV1の結果と似ている。

28 **Physical conditions in the warped accretion disk of a massive star. 349 GHz ALMA observations of G023.01−00.41**

A. Sanna, A. Giannetti, M. Bonfand, L. Moscadelli, R. Kuiper, J. Brand, R. Cesaroni, A. Caratti o Garatti, T. Pillai, K. M. Menten

Young massive stars warm up the large amount of gas and dust which condenses in their vicinity, exciting a forest of lines from different molecular species. Their line brightness is a diagnostic tool of the gas physical conditions locally, which we use to set constraints on the environment where massive stars form. We made use of the Atacama Large Millimeter/submillimeter Array at frequencies near 349 GHz, with an angular resolution of $0.1''$, to observe the methyl cyanide (CH_3CN) emission which arises from the accretion disk of a young massive star. We sample the disk midplane with twelve distinct beams, where we get an independent measure of the gas (and dust) physical conditions. The accretion disk extends above the midplane showing a double-armed spiral morphology projected onto the plane of the sky, which we sample with ten additional beams: along these apparent spiral features, gas undergoes velocity gradients of about $1 kms^{-1}$ per 2000 au. The gas temperature (T) rises symmetrically along each side of the disk, from about 98 K at 3000 au to 289 K at 250 au, following a power law with radius, $R^{-0.43}$. The CH_3CN column density (N) increases from $9.2 \times 10^{15} cm^{-2}$ to $8.7 \times 10^{17} cm^{-2}$ at the same radii, following a power law with radius, $R^{-1.8}$. In the framework of a circular gaseous disk observed approximately edge-on, we infer an H_2 volume density in excess of $4.8 \times 10^{9} cm^{-3}$ at a distance of 250 au from the star. We study the disk stability against fragmentation following the methodology by Kratter et al. (2010), appropriate under rapid accretion, and we show that the disk is marginally prone to fragmentation along its whole extent.

CH3CNを使ったmassive star G023.01-00.41の円盤の観測

・CH_3CNを使う利点

数GHzの狭い領域に、励起温度が数100Kに渡る多くのラインがある

$CH_3{}^{13}CN$のラインも同じ領域で観測可能

H_2密度 $>10^5 cm^3$で有効な温度のトレーサー

・massive star G023.01-00.41

距離：4.59 kpc

$10^{4.6}$ Lsun, 20Msun のZAMS

先行研究で3000 auの円盤構造が見えている。

infall gas の降着率は6×10^{-4} Msun

円盤はi<30° でほぼ edge on

ALMAを用いてCH_3CNとCH_3OHを観測

円盤の物理構造を調べる。

（右図）

円盤構造とそれに付随する腕構造が見える

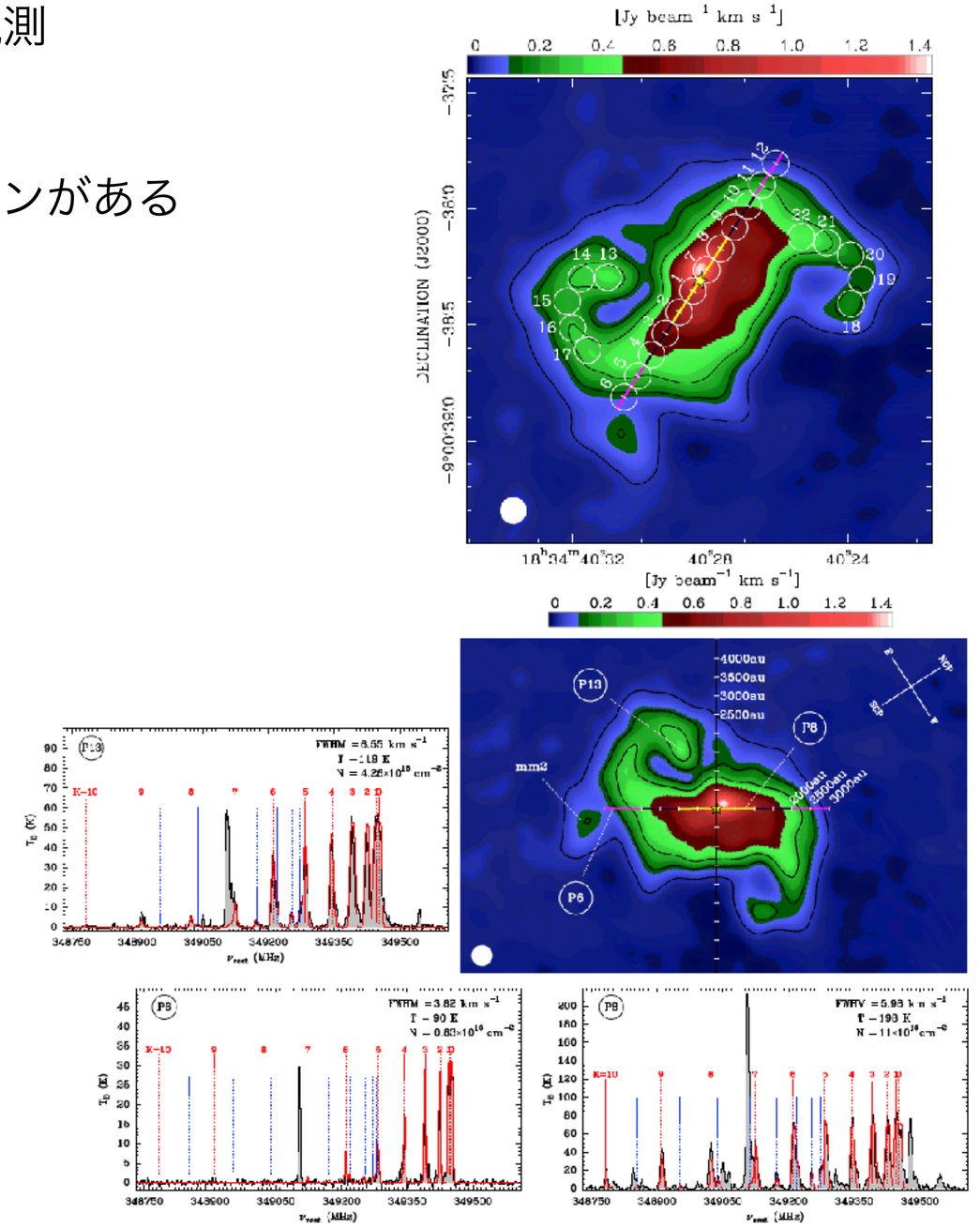

円盤の物理構造

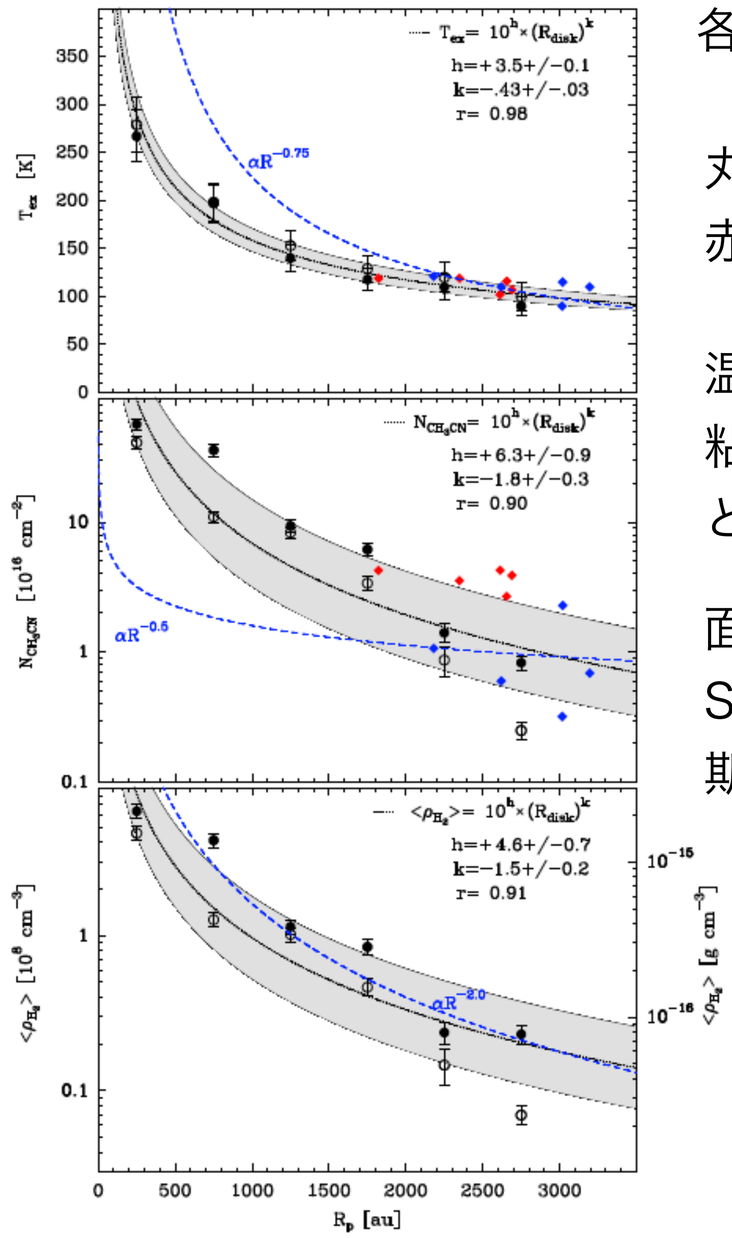

各lineの情報からMCMCを用いて計算

丸印が円盤の赤道面での値
赤と青のひし形が腕構造での値

温度分布は冪が~-4.3となり、
粘性降着円盤で実現する値（3/4）
と比べて緩やか

面密度分布の冪は-1.8
Shu 的な定常降着のエンベロープで
期待される-0.5に比べて緩やか

視線上で平均した密度
赤道面の最大密度は
これより大きくなる

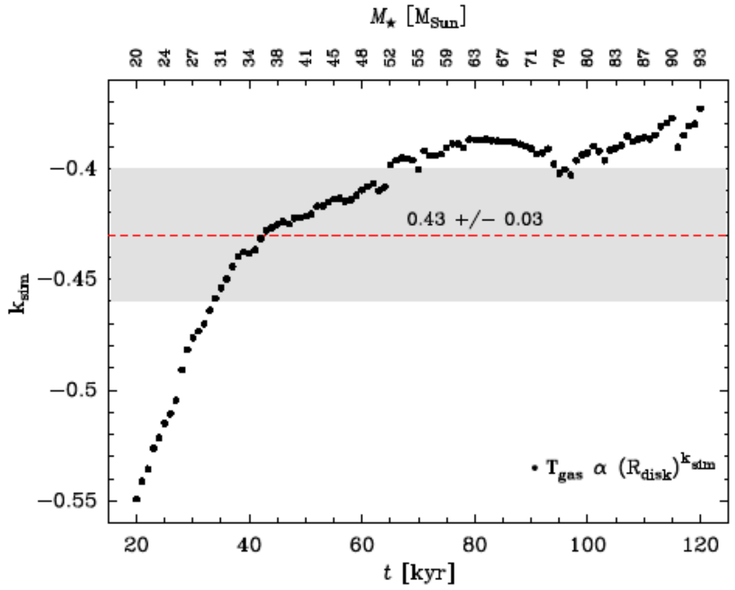

massive star 形成のシミュレーション（Kuiper and Hosokawa 2018）との温度の冪の比較。
形成過程で冪~-4となるのは
シミュレーションと整合的

自己重力不安定で分裂するか？
Kratter + 2010で得られた経験則と比較

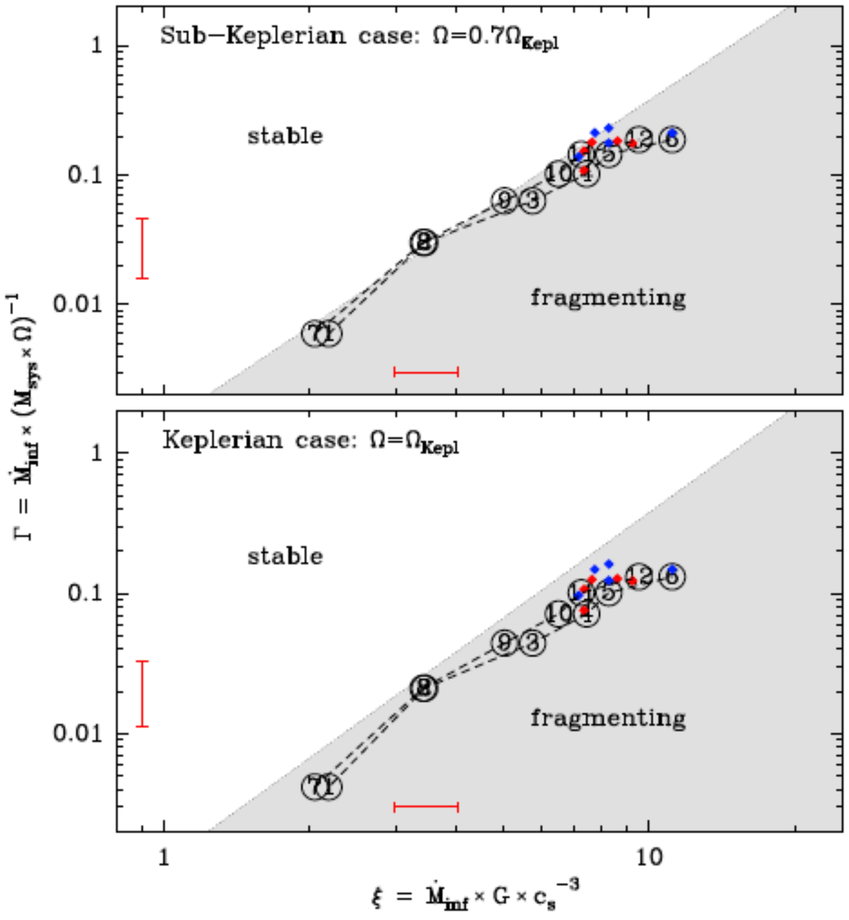

各場所での無次元パラメータΓ、ξを分裂条件と比較
数字は赤道面状の場所に対応。スパイラル構造は青と赤の印。

marginal に分列する領域にいるので、伴星が形成可能か？
高分解能観測で構造が見えるかもしれない

（注）
Kratter+ 2010 では、このパラメータは一つの系に対して1組決まる。
（Ωは円盤にinfall してきているガスの角速度。
　また、Kratter+ 2010 は等温の計算）
この論文では各半径で見積もっている。
結果の解釈は注意が必要
（Ωをover estimate しているせいで分裂しそうに見える？）

円盤はほぼedge on, 腕構造は円盤の上下方向に伸びている。
→重力不安定でできる渦状腕というより、infall しているガスを見ている

29 # FORCAST imaging of two small nearby Clusters: The Coronet and B59

G. Sandell, B. Reipurth, W. D. Vacca, N. S. Bajaj

We present mid infrared imaging of two young clusters, the Coronet in the CrA cloud core and B59 in the Pipe Nebula, using the FORCAST camera on the Stratospheric Observatory for Infrared Astronomy. We also analyze Herschel Space Observatory PACS and SPIRE images of the associated clouds. The two clusters are at similar, and very close, distances. Star formation is ongoing in the Coronet, which hosts at least one Class 0 source and several pre-stellar cores, which may collapse and form stars. The B59 cluster is older, although it still has a few Class I sources, and is less compact. The CrA cloud has a diameter of about 0.16 pc, and we determine a dust temperature of 15.7 K and a star formation efficiency of about 27 twice as large, has a dust temperature of about 11.4 K and a star formation efficiency of about 14 the Coronet, which has also formed intermediate mass stars, while B59 has only formed low-mass stars.

30 **Chandra X-ray Observations of V830 Tau: A T Tauri Star Hosting an Evanescent Planet**

Stephen L. Skinner, Manuel Guedel

A radial velocity study by Donati et al. (2016) reported the detection of a close-in giant planet in a 4.93 d orbit around the 2 Myr old weak-lined T Tauri star V830 Tau. Because of the stringent timescale constraints that a very young host star like V830 Tau would place on hot Jupiter formation models and inward migration mechanisms, independent confirmation of the planet's existence is needed but so far has not been obtained. We present new Chandra X-ray observations of V830 Tau. The Chandra observations in combination with previous XMM-Newton observations reveal strong variable X-ray emission with an X-ray luminosity spanning the range log Lx = 30.10 - 30.87 ergs/s. Chandra High Energy Transmission Grating (HETG) spectra show emission lines formed over a range of plasma temperatures from 4 MK (Ne IX) to 16 MK (S XV). At the separation of the reported planet (0.057 au) the X-ray flux is 10^6 - 10^7 times greater than the Sun's X-ray flux at Jupiter. We provide estimates of the X-ray ionization and atmospheric heating rates at the planet's separation and identify areas of uncertainty that will need to be addressed in any future atmospheric models.

31 # X-raying the Sco-Cen OB association: The low-mass stellar population revealed by eROSITA

J. H. M. M. Schmitt, S. Czesla, S. Freund, J. Robrade, P. C. Schneider

We present the results of the first X-ray all-sky survey (eRASS1) performed by the eROSITA instrument on board the Spectrum-Roentgen-Gamma (SRG) observatory of the Sco-Cen OB association. Bona fide Sco-Cen member stars are young and are therefore expected to emit X-rays at the saturation level. The sensitivity limit of eRASS1 makes these stars detectable down to about a tenth of a solar mass. By cross-correlating the eRASS1 source catalog with the Gaia EDR3 catalog, we arrive at a complete identification of the stellar (i.e., coronal) source content of eROSITA in the Sco-Cen association, and in particular obtain for the first time a 3D view of the detected stellar X-ray sources. Focusing on the low-mass population and placing the optical counterparts identified in this way in a color-magnitude diagram, we can isolate the young stars out of the detected X-ray sources and obtain age estimates of the various Sco-Cen populations. A joint analysis of the 2D and 3D space motions, the latter being available only for a smaller subset of the detected stellar X-ray sources, reveals that the space motions of the selected population show a high degree of parallelism, but there is also an additional population of young, X-ray emitting and essentially cospatial stars that appears to be more diffuse in velocity space. Its nature is currently unclear. We argue that with our procedures, an identification of almost the whole stellar content of the Sco-Cen association will become possible once the final Gaia and eROSITA catalogs are available by the end of this decade. We furthermore call into question any source population classification scheme that relies on purely kinematic selection criteria.

32 The filamentary structures in the CO emission toward the Milky Way disk

J. D. Soler, H. Beuther, J. Syed, Y. Wang, Th. Henning, S. C. O. Glover, R. S. Klessen, M. C. Sormani, M. Heyer, R. J. Smith, J. S. Urquhart, J. Yang, Y. Su, X. Zhou

We present a statistical study of the filamentary structure orientation in the CO emission observations obtained in the Milky Way Imaging Scroll Painting (MWISP) survey in the range $25.8\,\mathrm{deg} < l < 49.7\,\mathrm{deg}$, $|b| \leq 1.25\,\mathrm{deg}$, and $-100 < v_{\mathrm{LSR}} < 135$ km/s. We found that most of the filamentary structures in the ^{12}CO and ^{13}CO emission do not show a global preferential orientation either parallel or perpendicular to the Galactic plane. However, we found ranges in Galactic longitude and radial velocity where the ^{12}CO and ^{13}CO filamentary structures are parallel to the Galactic plane. These preferential orientations are different from those found for the HI emission. We consider this an indication that the molecular structures do not simply inherit these properties from parental atomic clouds. Instead, they are shaped by local physical conditions, such as stellar feedback, magnetic fields, and Galactic spiral shocks.

33

The general applicability of self-similar solutions for thermal disc winds

Andrew D. Sellek, Cathie J. Clarke, Richard A. Booth

Thermal disc winds occur in many contexts and may be particularly important to the secular evolution and dispersal of protoplanetary discs heated by high energy radiation from their central star. In this paper we generalise previous models of self-similar thermal winds - which have self-consistent morphology and variation of flow variables - to the case of launch from an elevated base and to non-isothermal conditions. These solutions are well-reproduced by hydrodynamic simulations, in which, as in the case of isothermal winds launched from the mid-plane, we find winds launch at the maximum Mach number for which the streamline solutions extend to infinity without encountering a singularity. We explain this behaviour based on the fact that lower Mach number solutions do not fill the spatial domain. We also show that hydrodynamic simulations reflect the corresponding self-similar models across a range of conditions appropriate to photoevaporating protoplanetary discs, even when gravity, centrifugal forces, or changes in the density gradient mean the problem is not inherently scale free. Of all the parameters varied, the elevation of the wind base affected the launch velocity and flow morphology most strongly, with temperature gradients causing only minor differences. We explore how launching from an elevated base affects Ne II line profiles from winds, finding it increases (reduces) the full width at half maximum (FWHM) of the line at low (high) inclination to the line of sight compared with models launched from the disc mid-plane and thus weakens the dependence of the FWHM on inclination.